

Do trout swim better than eels? Challenges for estimating performance based on the wake of self-propelled bodies

Eric D. Tytell

Received: 12 February 2007 / Revised: 16 May 2007 / Accepted: 4 June 2007 / Published online: 28 June 2007
© Springer-Verlag 2007

Abstract Engineers and biologists have long desired to compare propulsive performance for fishes and underwater vehicles of different sizes, shapes, and modes of propulsion. Ideally, such a comparison would be made on the basis of either propulsive efficiency, total power output or both. However, estimating the efficiency and power output of self-propelled bodies, and particularly fishes, is methodologically challenging because it requires an estimate of thrust. For such systems traveling at a constant velocity, thrust and drag are equal, and can rarely be separated on the basis of flow measured in the wake. This problem is demonstrated using flow fields from swimming American eels, *Anguilla rostrata*, measured using particle image velocimetry (PIV) and high-speed video. Eels balance thrust and drag quite evenly, resulting in virtually no wake momentum in the swimming (axial) direction. On average, their wakes resemble those of self-propelled jet propulsors, which have been studied extensively. Theoretical studies of such wakes may provide methods for the estimation of thrust separately from drag. These flow fields are compared with those measured in the wakes of rainbow trout, *Oncorhynchus mykiss*, and bluegill sunfish, *Lepomis macrochirus*. In contrast to eels, these fishes produce wakes with axial momentum. Although the net momentum flux must be zero on average, it is neither spatially nor temporally homogeneous; the heterogeneity may provide an alternative route for estimating thrust. This review shows examples of wakes and velocity profiles from the three fishes, indicating challenges in estimating efficiency and power output and suggesting several routes for further

experiments. Because these estimates will be complicated, a much simpler method for comparing performance is outlined, using as a point of comparison the power lost producing the wake. This wake power, a component of the efficiency and total power, can be estimated in a straightforward way from the flow fields. Although it does not provide complete information about the performance, it can be used to place constraints on the relative efficiency and cost of transport for the fishes.

1 Introduction

Fishes are often assumed to be highly efficient swimmers. After all, many species routinely swim or migrate over very long distances, including fishes of such diverse shapes and sizes as eels, tunas, many sharks, and river fishes like trout (Helfman et al. 1997). Natural selection has had hundreds of millions of years (Helfman et al. 1997) to tune the design of these fishes. One would naturally imagine that efficient swimming would be an important design criterion, particularly for these migratory or long-distance swimmers. Therefore, biologists and engineers have been eager to examine the efficiency of undulatory swimming, with a goal of determining the best fish body shapes and swimming modes, and to extract design principles for the construction of highly efficient underwater autonomous vehicles.

This goal, however, is based on a fallacy. Natural selection has *not* produced optimal swimming performance. Selection merely results in performance that is good enough that an animal can avoid dying or being eaten long enough to reproduce (Garland 1998). “Good enough,”

E. D. Tytell (✉)
Department of Biology, University of Maryland,
College Park, MD 20742, USA
e-mail: tytell@umd.edu

also, is determined within a multitude of conflicting demands. Evolutionary history, feeding, migration, and sexual displays, among many other factors, all simultaneously influence an organism's fitness. Not only this, but the conditions under which selection happens are constantly changing, as predators and prey evolve together and the environment changes. Even though any one fish species is not optimal (or even necessarily very good), the differences among species may provide useful hints for the design of underwater vehicles.

However, it would be wise not to assume that fish swimming is highly efficient—it might not be, particularly in comparison to propeller-based propulsion at steady speeds. For a migrating fish, an independent and possibly more important criterion than efficiency is energy consumption. The hydrodynamic energy consumption rate P_{total} is composed of two components,

$$P_{\text{total}} = UT + P_{\text{waste}}, \quad (1)$$

where UT is the useful power, the product of swimming velocity U and the thrust force T , and P_{waste} is the wasted power. For the purposes of this review, P_{waste} is assumed to be only the power used to produce a wake (P_{wake}); metabolic power wasted converting chemical energy into mechanical energy is ignored. Propulsive efficiency, in turn, is conventionally defined as

$$\eta = UT/P_{\text{total}}. \quad (2)$$

Based on these definitions, P_{total} could be large, even if η is close to one. For example, a fish with high drag might put 99% of its locomotory energy to forward propulsion, but end up using more total energy than a very streamlined fish that wastes 50% of its output.

Together, however, propulsive efficiency and total energy output provide a useful way of comparing the swimming performance of different fishes and underwater vehicles. While natural selection cannot be said to produce optima, different species of fishes presumably differ in propulsive efficiency or total power consumption. In particular, one would expect migratory fishes, like trout, and eels, to be better swimmers than fishes that generally stay put, like bluegill sunfish—although the criteria that determine “better” are unknown. As an evolutionary question, it would be interesting to examine those criteria. How does hydrodynamic performance factor into the shape changes over the evolutionary history of fishes? For example, trout and eels, two very differently shaped fishes, both swim long distances—is one body shape more efficient or more power-conserving than the other? Or are other factors, unrelated to swimming, more important in determining body shape? As an engineering question, it would also be

useful to compare swimming performance among different types of self-propelled systems. If one wanted to design a submarine, would it be better be shaped like a trout, an eel, or a conventional propeller-based underwater vehicle?

The recent availability of high-resolution, high-speed particle image velocimetry (PIV; Willert and Gharib 1991) systems has made it possible and relatively straightforward to measure the fluid flow in a two-dimensional plane around swimming fishes (e.g., Anderson et al. 2001; Müller et al. 1997; Nauen and Lauder 2002a; Tytell and Lauder 2004). This measurement technique has raised the possibility of estimating the thrust or drag on a swimming fish from the flow in its wake. To date, however, such estimates have been problematic (Schultz and Webb 2002).

In this review, the differences among wakes of several swimming fishes are first demonstrated, using examples from swimming eels (Tytell 2004a; Tytell and Lauder 2004), along with rainbow trout and bluegill sunfish (E. D. Tytell, unpublished data). These differences are examined by looking at the net momentum flux in each wake. Because thrust is problematic to estimate in general, the wake power is instead studied. Although it is only one component of the total power, this review demonstrates how it can be used to bracket the possible performance envelopes of different fishes for future comparative studies.

1.1 Swimming modes

The fishes examined in this review span much of the range of the standard classification of swimming modes (Breder 1926). Eels are termed anguilliform swimmers, and are understood to undulate with about one complete wave on their bodies, with a substantial undulation amplitude even close to the head. Bluegill sunfish, in contrast, are termed carangiform swimmers, and bend through about half of a wave, which only reaches a substantial amplitude in the posterior third of their bodies. Trout are called subcarangiform, which is intermediate between the eel and the bluegill.

Additionally, the fish span a range of body shapes. Eels are elongate, with a fairly constant oval cross-section and no physical demarcation between the “tail” and “body.” Bluegill, in contrast, have a highly flattened body with a fairly separate tail (caudal fin), joined by a narrow region termed the caudal peduncle. Trout, again, are intermediate, with a fusiform body and separate tail, but less narrowing at the caudal peduncle than bluegill.

Figure 1 shows examples of the kinematics and body shape for each fish. Although the eel moves its anterior body more than the other fishes, all fishes have some head motion. In fact, the modes are more similar than they are different (Lauder and Tytell 2006). Specifically, both the

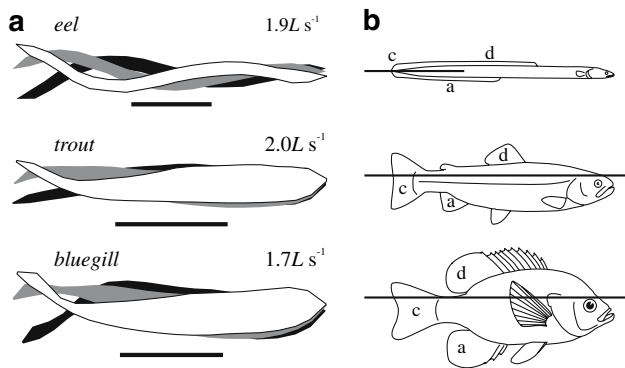


Fig. 1 Kinematics and body shapes for each of the example fishes. **a** Silhouettes of the fishes swimming at approximately the same length (L) specific speeds [eel data from Tytell (2004a); trout and bluegill from E. D. Tytell, unpublished data]. Tracings are shown for three instants, separated by the same amount of time, between maximum lateral tail tip excursion on either side. Scale bars are all 5 cm. **b** Line drawings of the fishes, showing the differences in body shape. Approximate positions and extents of the PIV measurement planes are shown with a thick line. For reference, the median fins are identified by letter (c caudal fin, d dorsal fin, a anal fin). In the eel, the three fins are joined. The dorsal and anal fins are shown fully erect, but are often lowered during steady swimming, particularly at higher speeds

angle of the tail and amplitude of its motion, which together probably determine the majority of the thrust (Lighthill 1960), are very similar for all of the modes. Despite the similarities in the kinematics, the differences in three-dimensional body shape (Fig. 1b) may result in different wake flow (Tytell 2006).

2 Wake flow

Early observations of the flow in the wake of swimming fishes showed the presence of a reverse von Kármán vortex street (Anderson 1996; McCutchen 1977; Müller et al. 1997; Rosen 1959). Sets of staggered vortices are arrayed in the wake, with jets in between them pointing laterally and along the swimming direction (axially), away from the animal. This structure is indicative of thrust production (Koochesfahani 1989; Triantafyllou et al. 1993). Eels were later shown to have a somewhat different wake structure, with two pairs of counter-rotating vortices shed per tail beat (Müller et al. 2001; Tytell and Lauder 2004), and very little net axial flow.

Examples for these two types of wake during swimming at about 1.9 body lengths (L) per second are shown in Fig. 2. The eel wake is modified from Tytell (2004a) and the bluegill wake is from previously unpublished data, gathered in the same flow tank under similar conditions and analyzed using the same custom Matlab PIV code (Mathworks, Natick, MA, USA; see Tytell and Lauder 2004, for a detailed explanation of methods). All animal procedures

were approved by the Harvard University Institutional Animal Care and Use Committee.

The flow in the eel's wake (Fig. 2a) is concentrated into jets with predominately lateral flow, and are separated by pairs of same-sign vortices or a shear layer (e.g., between jets 1 and 2 in Fig. 2a). In contrast, flow in the wake of a bluegill sunfish (Fig. 2b) contains jets with a distinct axial component (particularly the fully formed jet 2; Fig. 2b), and the jets are separated by a single vortex.

Why are the wakes so different? In both cases, the animals were swimming quite steadily, holding station against the flow (38 cm s^{-1} for the eel; 27 cm s^{-1} for the bluegill) while drifting $<1 \text{ cm}$ in the laboratory frame of reference over four tail beats. Thus, for both fishes, the net force remains close to zero when averaged over many tail beats. This does not mean, however, that the net force is necessarily zero at any specific instant in time. If thrust is produced in a much more pulsatile way than drag, then it may periodically overwhelm the drag, resulting in a center-of-mass acceleration and a corresponding momentum flux in the wake. This effect will be termed “temporal separation” of thrust and drag.

If thrust and drag are separated temporally, then the center-of-mass speed should fluctuate. Center of mass was therefore estimated on the basis of height and width profiles by assuming the fish's bodies have a constant density and oval cross-section. Figure 3 shows the instantaneous center-of-mass speed and the tail position. Velocities were determined from video using the technique detailed in Tytell and Lauder (2004), which is based on a smoothing-spline method evaluated in Walker (1998). Both framing rate and magnification were the same for all data (250 frames per second, and about 300 pixels per body length), which should result in comparable error on the velocity estimates (Walker 1998).

All three species show velocity oscillations at least at twice or possibly at four times the tail beat frequency. Eels maintain the smoothest velocity trace (Fig. 3a), with root-mean-squared (RMS) velocity fluctuations about the mean of about $0.03 L \text{ s}^{-1}$ (5 mm s^{-1}) for this sequence, consistent with their nearly zero-momentum wakes. Trout have fluctuations of $0.07 L \text{ s}^{-1}$ (10 mm s^{-1}) (Fig. 3b). Bluegill have the largest oscillations, $\sim 0.09 L \text{ s}^{-1}$ (15 mm s^{-1}) about the mean (Fig. 3c), which suggests that their wakes should show corresponding fluctuations in net momentum.

A second possible reason that the wakes differ may be because of the differences in body shape. Over the course of many tail beats, the fish maintain a consistent orientation to the oncoming flow, indicating that the average forces through a tail beat must integrate to zero over the body's surface. This does not mean, however, that the force is necessarily zero at any given point on the body. In particular, for the bluegill and trout, the anterior body

Fig. 2 Representative wake vector fields for the eel (**a**), modified from Tytell and Lauder (2004), with an additional flow field for the bluegill sunfish (**b**). Fluid flow direction and magnitude is indicated with *arrows*. In panel **a**, every other vector is skipped for clarity. *Scale bars and scale vectors* are shown below and are the same for both panels. Vorticity magnitude is given with shades of *gray*; note that the scales are different for panels **a** and **b**. The outline of the tail is shown in *gray* at the top of each panels. Due to the shadow from the tail, some vectors could not be calculated and are not shown. The position of downstream velocity transects is indicated by a *box*, and the jets are identified with the *numbers 1 and 2*

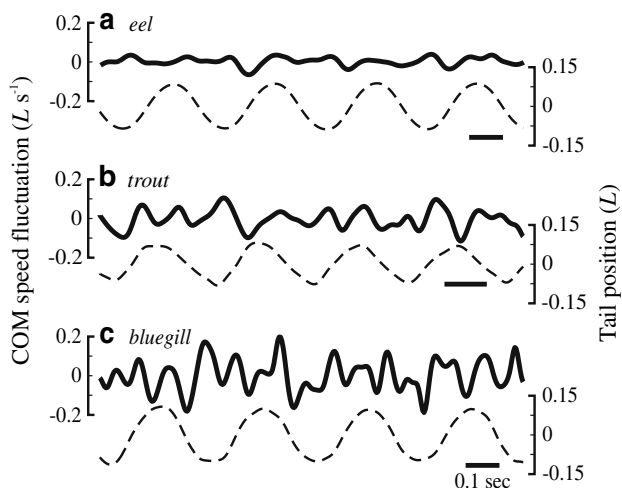
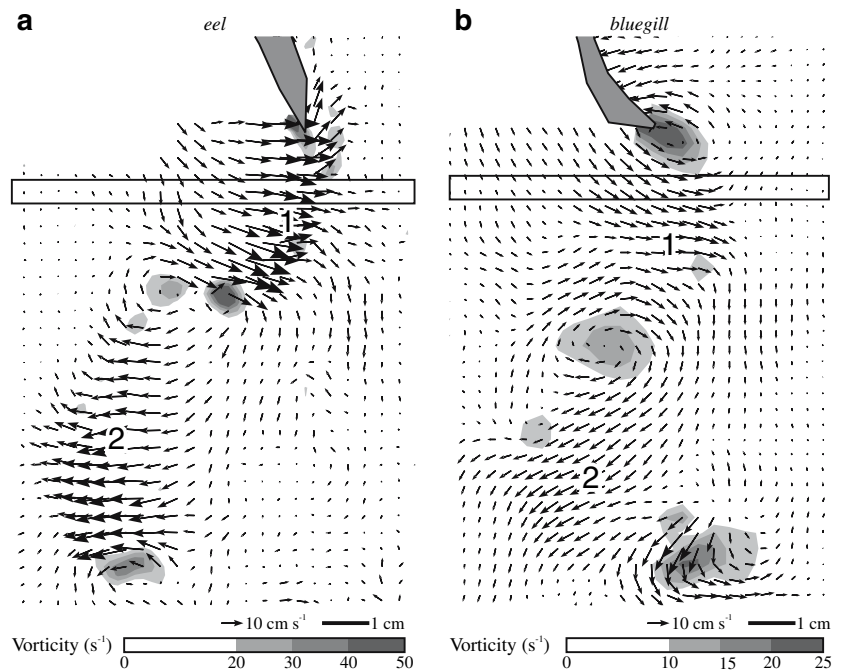


Fig. 3 Representative traces of the fluctuations of the axial center-of-mass speed around the mean swimming speed (*solid line, left axes*) and the lateral position of the tail tip relative to the mean body position (*dashed line, right axes*), for each of the three fishes. Each trace is from a swimming speed of $\sim 1.9 L s^{-1}$. *Horizontal scale bars* are all 0.1 s

probably contributes most of the drag and relatively little thrust, while the tail contributes mostly thrust with relatively little drag. The body drag appears not to strongly affect the flow encountered by the tips of the tail, because low-momentum flow from the body does not separate, but rather converges on the center line as the peduncle narrows (Anderson et al. 2001; Nauen and Lauder 2001). This effect will be termed “spatial separation” of thrust and drag. For the eel, in contrast, spatial separation of forces is

probably much less significant, with much of the body contributing to both thrust and drag. Simulations of anguilliform swimming by Kern and Koumoutsakos (2006) support this idea. Their calculations indicated that substantial thrust in eels may be produced by segments anterior to the tail (Kern and Koumoutsakos 2006), unlike in carangiform swimmers.

2.1 Control volume analysis

To examine both spatial and temporal separation of forces, it is best to use a standard control volume analysis (see any fluid dynamics textbook; e.g., Shames 1992) in a cubic region surrounding the fish. The animal produces forces, first, by altering the pressure locally, and second, by changing the fluid momentum. The total force is estimated by integrating the pressure over the surface of the volume and the momentum flux through the surface.

One substantial challenge of these analyses is that techniques like PIV cannot measure pressure directly. The standard way to deal with this issue is to place the sides of the control volume sufficiently far away from the fish that local changes in pressure are converted to fluid acceleration and the pressure on the sides of the control volume is ambient. This method has two problems. First, measurement techniques are often limited in spatial resolution. Examining a large area thus means fewer measurements directly in the wake, where the flows are complex. Second, the further away measurements are made, the more diffuse the wake becomes due to both viscous and turbulent effects (see Tytell and Ellington

2003, for a detailed discussion of these effects). More precision is thus necessary for measurements in the far wake than for those in the near wake.

However, because fishes are self-propelled, they may not require such large control volumes. The net force is close to zero, and so any local pressure changes will be small and will be distributed in the wake quite rapidly. Consider the changes in velocity shown in Fig. 3. Peak acceleration for the bluegill is around $2,000 \text{ mm s}^{-2}$, corresponding to a force of about 150 mN for the $\sim 70 \text{ g}$ fish. Remember, this force is not thrust, but a rough estimate of the peak net force. If all of this force is due to pressure applied to an actuator surface swept out by the tail over a tail beat, then the pressure change on that surface would be well under 1% of ambient. Thus, due to the very low-net forces on a self-propelled body, pressure changes even in the near wake can safely be neglected.

For the control volume analysis, the remaining effect is momentum flux through the sides of the volume. If the sides and the top and bottom are placed parallel to the mean flow and sufficiently far from the wake, they will have zero flux. In the end, the only planes that matter are the transects upstream and downstream of the fish.

Since the fluid density and mean flow speed are constant, the momentum flux through these planes is proportional to the average net fluid velocity added by the fish. Transects across the wake were therefore estimated in a 5 mm thick box spanning the wake, placed 10 mm downstream from the average tail position (examples shown in Fig. 2). Single transects were produced by averaging the PIV vectors along the axial thickness of the box, which helped to reduce noise. If necessary, transects were angled to be perpendicular to the swimming angle of the fish to compensate for any small angle that might have been present. Swimming angle was $<2^\circ$ on average.

The net momentum flux is the difference between the flux through the upstream and downstream planes of the control volume. For trout and bluegill, upstream flow was measured directly and upstream transects were estimated analogously to the wake transects, but placed 10 mm upstream from the head. For eels, upstream flow could not be measured directly, because the animals would not swim consistently with their heads in the laser light sheet (Tytell and Lauder 2004). Instead, the laser light sheet was positioned to view flow around the posterior two thirds of the eels' bodies (Fig. 1), and flow entering the control volume was estimated from the average flow field measured without an animal present.

Figure 4 shows net fluid flow in the eel wake during swimming at 1.9 L s^{-1} , corresponding to a Reynolds number of 80,000 based on body length. Figure 4a shows transects at three phases, with the left half of the tail beat (thin solid lines) superimposed on the mirror image of the

right half (thin dashed lines) to show the symmetry of the tail beat. Phase-averaged flow profiles are shown with thick lines. In the 410 flow fields analyzed in this sequence, the net velocity averaged across the transect never deviated more than 9% from the mean flow speed (indicated by the bars on the right in Fig. 4). The mean velocity in the phase-averaged profiles (triangles on the right of Fig. 4a), in turn, was less than the measurement error, and thus indistinguishable from zero. At each point in time, therefore, measurements suggest that the eel wake has close to zero net momentum (as Tytell 2004a found through a different method).

The lack of net momentum, however, does not mean that the eel wake is strictly momentumless. Momentumless wakes are a special class of wakes produced by self-propelled bodies, when the thrust and drag forces are identically equal (Tennekes and Lumley 1972). Such wakes scale differently than drag or thrust wakes (Afanasyev 2004; Sirviente and Patel 2000; Tennekes and Lumley 1972). The wake structure is very sensitive to any deviation from precisely zero net force (Meunier and Spedding 2006). The eel's wake averaged over a full tail beat (Fig. 4b) is reminiscent of the classic mean velocity profile in a momentumless jet (Tennekes and Lumley 1972) and has a similarly strong sensitivity to small deviations from zero-net force (Tytell 2004b). The eel's wake, though turbulent, differs from experimental studies of self-propelled turbulent jets (Finson 2006; Naudascher 1965; Sirviente and Patel 2000) in that the vortices are more coherent and the time scales are longer. Thus, the eel's wake is probably not truly momentumless, particularly in how wake velocity and turbulence scale with distance from the fish, because net momentum fluctuates around zero (indicated by the bars in Fig. 4a), and the center-of-mass velocity oscillates accordingly. However, it is possible that general conclusions from these jet studies, such as the spatial separation of thrust and drag profiles suggested by Sirviente and Patel's (2000) results, can be applied to the eel's wake.

Trout and bluegill wakes, in contrast, clearly do contain net momentum (Fig. 5), at least in the plane in which PIV was conducted. At nearly every point in the cycle, the phase-averaged wakes for both fishes have non-zero momentum flux (Fig. 5a, c). Bluegill have a wake with net momentum above zero at almost every phase in the tail beat cycle (ranging from -2 to 11% of the free-stream momentum flux; Fig. 5c) and on average throughout the tail beat (about 5% of free stream; Fig. 5d). Trout have less net momentum than bluegill, with some instantaneous transects near zero (range -4 – 13% of free stream; bars on right in Fig. 5a). The average wake for trout (Fig. 5b) also resembles a momentumless wake profile, with one center peak with momentum above free-stream and two side lobes with momentum below free-stream (Tennekes and Lumley

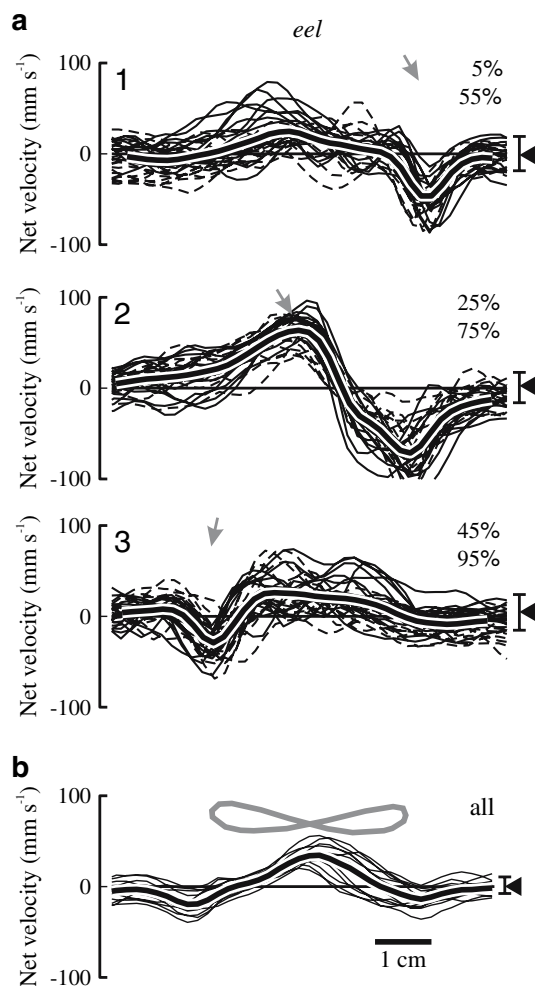


Fig. 4 Transsects of axial velocity in the eel's wake during swimming at $1.9 L s^{-1}$ in a region 10–15 mm downstream of the tail, showing axial velocity (*thin lines*), the phase averaged transect (*thick line*), and the position and angle of the tail (*gray arrows or line*). The *bar* on the right indicates the range of mean velocities taken from each transect, and mean velocity across the phase averaged transect is shown with a *triangle*. **a** Transsects at particular phases (given by percentages in the *upper right*) during the tail beat cycle. Transsects in which the tail is moving from *right to left* (*solid lines*) have been mirrored and superimposed on left-to-right transects (*dashed lines*), centering on the tail position. The lateral tail position and angle is indicated with a *gray arrow*. The overall phase average is shown with a *thick line* outlined in *white*. **b** Mean transects over the entire tail beat. Transects are centered on the mean tail position, and the path of the tail is shown in *gray*. The mean over all tail beats is shown with a *thick line* outlined in *white*. Scale bar at bottom is 1 cm and is valid for all plots

1972), but the net momentum is nonetheless slightly above zero (about 2% of the free-stream momentum flux).

These transects are examples of the differences between anguilliform, subcarangiform, and carangiform wakes, and have not been subjected to the statistical analysis necessary to discern real differences between the classes of wakes independently from differences among these particular individuals. However, the general structure is consistent

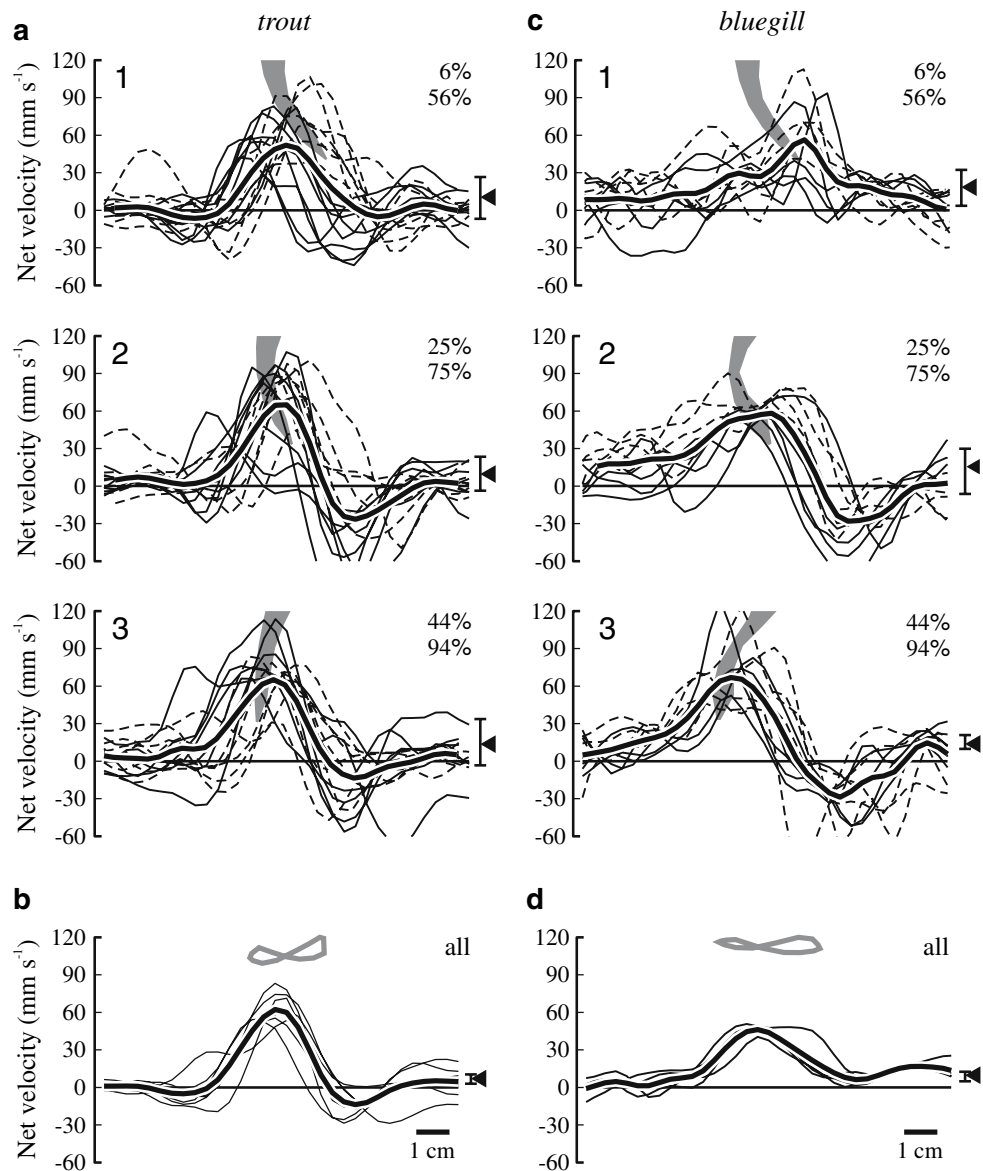
with previous, more detailed results (Drucker and Lauder 2001; Nauen and Lauder 2002b).

Why do the bluegill and trout wakes have net momentum? Although both animals have a fluctuating center-of-mass velocity (Fig. 3b, c), temporal separation of thrust and drag does not appear to be the cause of the net momentum in their wakes. If this were the case, one would expect the instantaneous momentum flux (Fig. 5a, c) to dip below zero at some times during the cycle and the average wake profiles (Fig. 5b, d) to have momentum integrals close to zero. Since neither effect is apparent, the more likely explanation is spatial separation of thrust and drag. Experimentally, the PIV plane was generally somewhat above or below the fish's midline (Fig. 1b). In bluegill, the upper and lower lobes of the caudal fin move faster and over a larger amplitude than the center of the fin (Lauder 2000; Tytell 2006), resulting in higher fluid velocities (Fig. 6) and likely more thrust than the center of the fin. Additionally, the body's drag will impact the upper and lower lobes of the tail less than the center. The drag reduces fluid momentum around the body, but, because flow does not separate on the body (Anderson et al. 2001; Nauen and Lauder 2001), the narrowing at the caudal peduncle will tend to cause the low-momentum fluid to converge on the fish's center line. Thus, if the measurement plane is somewhat off-center, the tail may appear to produce a thrust wake. In reality, thrust may genuinely be higher at the tail tips than at the center, due to the higher angle of attack of the tips (Lauder 2000; Tytell 2006) and possibly because of thrust enhancement due to interaction with vortices from the dorsal and anal fin (Drucker and Lauder 2001; Tytell 2006; Zhu et al. 2002), resulting in even more pronounced spatial separation of thrust and drag. However, streamwise tip vortices (Tytell 2006) may also reduce the thrust. A well-centered measurement plane might show a drag wake, but such detailed measurements have not been done. The best measurement would be a stereo-PIV (Prasad 2000) plane aligned perpendicular to the flow in the fish's wake.

2.2 Estimating thrust

Could these wake transects nonetheless be used to estimate thrust? For the eel, the challenge is extracting the thrust magnitude from a nearly zero momentum wake. This may be possible by measuring the height of the central peak in the average wake profile (Fig. 4b). Sirviente and Patel (2000) found that the peak in a momentumless wake close to the body has nearly the same maximum velocity and width as the thrust wake alone, and thus could be used to estimate the thrust force. However, it is not clear whether the same procedure could be used with the eel data to

Fig. 5 Transects through the trout and bluegill wakes during swimming at 2.0 and 1.7 $L s^{-1}$, respectively. Format of the plots is the same as in Fig. 4. **a, c** A silhouette of the tail is shown in gray



extract average thrust from an average wake profile, given that the turbulence in the wake is much more structured than in truly momentumless wakes (Meunier and Spedding 2006).

For the trout and bluegill, the challenge is different; the difficulty is in the spatial separation of thrust and drag. The velocity profile of a transect in a single plane (Fig. 5c, d) provides an estimate of the net force per unit height in that plane. Close to the tips of the tail, the net force is likely to be primarily thrust. However, thrust will not be homogeneous over the height of the tail, though, because the center moves slower and over a smaller amplitude than the tips (Lauder 2000; Tytell 2006) and hence has a lower angle of attack. Figure 6 shows that fluid velocities, and thus probably forces, at the upper and

lower lobes of the fin are about twice those at the center. Thus, it would be best to make measurements of momentum flux at the tips and the center of the tail over a range of speeds in which the tail beat amplitude varies. These measurements could be used to construct an empirical relationship between tail beat amplitude and momentum flux per unit height, which could then be used to estimate the total thrust at a single speed.

An alternative approach, used by many researchers, is to extract forces on the basis of the vortical structure of the wake (Drucker and Lauder 1999; Müller et al. 2001, 1997; Nauen and Lauder 2002a; Tytell 2004a). In this approach, vortices in the wake like those in Fig. 2b are assumed to link up in three dimensions to form a chain of linked vortex rings (e.g., Nauen and Lauder 2002a) or a series of separate

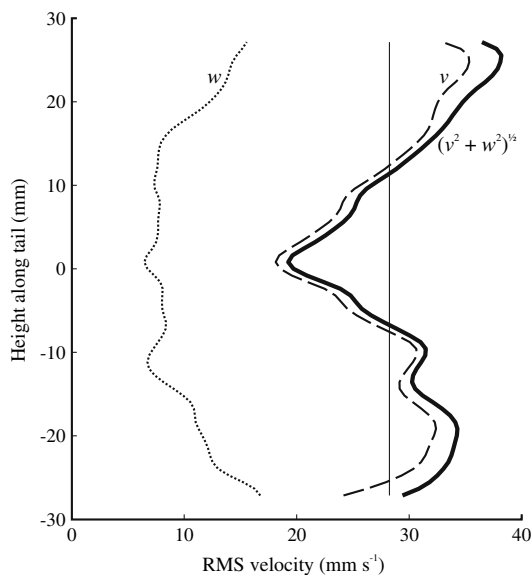


Fig. 6 Flow velocities in a transverse plane through the wake of the bluegill sunfish at different levels along the height of the tail (modified from Tytell 2006). Root-mean-squared (RMS) velocities are taken over the course of five tail beats, with lateral (v) velocities in the *dashed line*, vertical (w) velocities in the *dotted line*, and total velocities in the transverse plane in the *thick solid line*. The *thin vertical line* indicates the mean absolute velocity over the height of the tail. Note that the fluid flow at the upper and lower lobes of the tail has almost twice the velocity of the flow at the centerline

but interacting rings (e.g., Tytell and Lauder 2004). The standard expression for the impulse of an isolated, steadily traveling vortex loop (Batchelor 1973) is then used to estimate forces. This approach, though relatively common, has several potential deficiencies. First, the vortex rings are neither isolated nor steady. Recent work by Dabiri (2005, 2006) indicates that unsteady vortex rings have added mass, like that for solids, which can substantially alter the forces estimated by assuming an isolated, steadily moving vortex ring (Dabiri 2005). The effect of the linkage or interaction between the rings is unknown. Second, the rings are most likely not circular (Tytell 2006), and thus transmit forces to the fluid less efficiently than circular or even oval-shaped rings would (Lighthill 1970). Finally, turbulence can break up the assumed vortex structure, resulting in an underestimate of forces (Spedding et al. 1984; Tytell and Ellington 2003) unless all vortical structures are taken into account (Rosén et al. 2004). Validating this approach has been difficult. Drucker and Lauder (1999) found a good agreement between their thrust estimates for pectoral fin swimming (during which the fish holds its body straight) and the drag measured on an anesthetized fish. Nauen and Lauder (2002a), in contrast, did not find very good agreement. More experiments are necessary to validate this approach, probably using simulation or physical models (such as in Krueger and Gharib 2003; Tytell and Ellington 2003).

3 Wake power

A different approach, requiring fewer assumptions about the structure and temporal evolution of the wake is to estimate the net energy flux, or wake power, added by the fish. This approach was first advocated for biological research by Schultz and Webb (2002). To produce thrust, the fish that is not 100% efficient adds energy to the fluid in the form of the kinetic energy of the wake. PIV methods can conveniently measure the kinetic energy flux through a control volume surrounding the fish. In a low-turbulence flow tank, the upstream input is simply $1/2\rho h w U^3$, where U is the flow speed, h is the height of the fish, w is the width of the wake. Wake flow velocities can then be represented as $(U + u, v, w)$ where u , v , and w are the axial, lateral, and vertical fluid velocities produced by the fish, respectively. The net wake power is thus

$$P_{\text{wake}} = \frac{1}{2}\rho U \int [(U + u)^2 + v^2 + w^2 - U^2] dS, \quad (3)$$

where S is the downstream surface of the control volume. Simplifying the expression in the brackets to $2Uu + u^2 + v^2 + w^2$ helps to reduce round-off error when $U \gg u$.

Due to the use of standard two-dimensional PIV, vertical (w) velocities were not measured. For bluegill, the only fish for which such data exist, the w component is a fairly small fraction of the total velocity (data from Tytell 2006 replotted in Fig. 6). In this case, w is about 35% of v , on average, while u and v themselves are of comparable magnitude (e.g., see the flow field in Fig. 2b). Therefore, we assume that vertical velocities make a similarly small contribution to the total power in all three species of fish, and use a simplified form for power:

$$P'_{\text{wake}} = \frac{1}{2}\rho h U \int (2Uu + u^2 + v^2) dy, \quad (4)$$

where y is the coordinate of lateral position.

Equation (4) requires an assumption about the 3D profile of the wake, but makes no assumptions about the physics or temporal evolution of the wake, unlike the approaches described in §2.2. As written, the equation assumes uniform flow over the height of the wake, clearly an invalid assumption (as Fig. 6 shows). In the data used for this review, measurement planes were generally slightly above or below the dorso-ventral center line of the fish (Fig. 1), which appear to be the best level to make single-plane measurements, because those are where the mean intersects the measured velocities (Fig. 6). Planes at higher levels may overestimate the power. Measurement planes for the eel were well-centered at the dorso-ventral midline,

although they did not extend all the way anteriorly to the head (Fig. 1). Wake profiles at different levels are unknown for eels, but with a tapered and quite flexible caudal fin (Fig. 1b), it is likely that flow speeds will decrease away from the midline. Thus, the values from eels are probably also overestimates.

In all of these cases, it would be better to have parallel planes at multiple levels to assess the contribution of spatial variation in flow along the height of the fin. However, even one plane can provide useful information, although the data have to be regarded with appropriate caution, as indicated above.

Data analyzed included the entire American eel (*Anguilla rostrata*) data set from Tytell (2004a), consisting of 274 steady tail beats from three eels (body lengths from 20 to 23 cm) at swimming speeds from 0.5 to 2 $L s^{-1}$. Also analyzed were unpublished data including 27 tail beats from one trout (*Oncorhynchus mykiss*), body length 14 cm, swimming at 1, 2, and 2.5 $L s^{-1}$, and 31 tail beats from two bluegill sunfish (*Lepomis macrochirus*), lengths 15 and 16 cm, swimming at 1.25–2 $L s^{-1}$. Reynolds number ranges were from 20,000 to 80,000 for the eel, 20,000 to 50,000 for the trout, and 30,000 to 50,000 for the bluegill.

To compare the fishes, the data were normalized to produce a power coefficient C_p , analogous to a drag coefficient, by dividing by $\frac{1}{2}\rho S U^3$ (Krueger 2006; Schultz and Webb 2002; Tytell 2004a), where S is the wetted surface area for each species. The surface area was estimated from body width and height measurements, assuming an oval cross-section and including the caudal fin area. For eels, the estimated area was 0.18 L^2 ; for trout, 0.54 L^2 ; and for bluegill, 0.69 L^2 (close to the values estimated by Webb 1992). Note that this estimate does not include the dorsal or anal fins (Fig. 1). The wetted area (i.e., twice the lateral projected area) of these fins decreases with swimming speed: for bluegill, at the lowest speeds, they make up at most 0.10 L^2 (according to measurements in Standen and Lauder 2005), for trout they are about 0.006 L^2 (Standen and Lauder 2007), and for eels they are $\sim 0.02 L^2$ (E. D. Tytell, unpublished data).

Figure 7 shows mean wake power coefficients from eels, trout and bluegill at a range of swimming speeds. Eels maintain about the same power coefficient, about 0.004, over their range of swimming speeds, but with a fairly large spread (SD = 0.002). Below speeds of 2 $L s^{-1}$, both trout and bluegill have substantially higher power coefficients than eels (trout, 0.03; bluegill, 0.04). In the one high-speed swimming sequence from trout, the wake power coefficient dropped to 0.007.

This review is meant to demonstrate a technique of comparing swimming performance, and conclusions regarding differences between species should be considered tentative. With so few data, it is not possible to per-

form the appropriate statistical analyses to distinguish real differences among species from random variability among individuals. Nonetheless, the data do show some interesting trends. Bluegill sunfish waste the most energy during steady swimming, as might be expected, because they live in ponds or other relatively still bodies of water where they do not typically spend much time swimming steadily (Hartel et al. 2002). They may be better adapted to low-speed swimming and maneuvering, in which strict power conservation is not an important factor (Webb 2006). Trout have comparable power coefficients to bluegill at low and moderate speeds, but show a marked decrease in the wasted power coefficient at the highest speed examined, possibly reflecting their specialization for high-speed burst swimming, particularly while swimming upstream in rivers (as is known for a closely related species, Standen et al. 2004). Eels, often considered to be inefficient (Lighthill 1970), waste relatively much less power than bluegill or trout at the same swimming speeds.

The wake power is only one component of the total power (Eq. 1), but it can be used to set bounds on the useful power and the efficiency. For example, eels are generally thought to be less efficient than carangiform swimmers like trout (Lighthill 1970; but see van Ginneken et al. 2005). For the current data to be consistent with this hypothesis, the trout must, counterintuitively, expend much more total energy than the eel. Since it already wastes more energy, relative to its body shape, than the eel, it must expend even more useful energy overcoming drag, so that the wasted portion makes up a small fraction of the total. At the same speeds, the trout's wake power coefficient is about eight times larger than the eel's; to have the same propulsive efficiency at these speeds as the eel, its drag (=thrust) coefficient must also be eight times larger. Thus, it seems unlikely that trout are more efficient than eels at low swimming speeds, which is consistent with the metabolic data of van Ginneken et al. (2005).

In contrast, if one wanted to argue that the cost of transport for the trout was less than that for the eel swimming at the same speed, then the trout's drag coefficient would have to be much less than the eel's. In fact, if the eel's drag coefficient was less than the difference in the wake power coefficients, then the trout could never have a lower cost of transport. Of course, trout tend to swim faster than eels, and particularly tend to swim in bursts at high speeds, which could mean that their average cost of transport during intermittent swimming may be lower or equal to that of an eel swimming steadily at a low speed.

Webb has made a number of estimates of the drag and power output of swimming fishes, using a variety of techniques. He estimated the drag on swimming trout by measuring the maximum sustained swimming speeds of trout with artificially increased drag coefficients (Webb

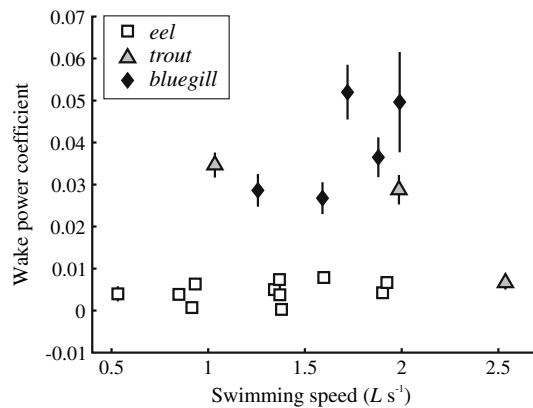


Fig. 7 Net wake power coefficients against swimming speed for eels (white squares), modified from Tytell (2004a), with additional data from bluegill (black diamonds) and trout (gray triangles) superimposed. Error bars indicate standard error. Where they are not visible, the symbol is larger than the error range

1971). In his study, he estimated a drag (=thrust) coefficient of ~ 0.05 over speeds from 1 to $2 L s^{-1}$. Together with the data in Fig. 7, this would indicate that trout have a hydrodynamic propulsive efficiency of about 60% at low speed, but about 85% at high speed. Webb (1992) also estimated useful power coefficients for both trout and bluegill sunfish using Lighthill's (1971) elongated body theory. This method suggested that the bluegill has a lower thrust power coefficient at low speeds than trout, but that they both approach 0.01 at higher speeds. Elongated body theory may not fully account for the forces in swimming (Tytell 2004a), but its underestimate is unlikely to be dramatically different for trout than bluegill. Thus, together with the current PIV data, these data suggest that bluegill are both more efficient and have a lower cost of transport than trout at low speeds, but that the trout is dramatically more efficient at higher speeds. These data seem to reflect the lifestyle and habitats of the fishes: still water and slow, irregular swimming for bluegill, but moving streams and fast burst swimming for trout.

One must be careful not to read too much into data like these. It is easy to construct “Just So” stories (after Kipling's 1907 stories for children) that explain exactly why the power coefficients should be the way they are. More data from more species are necessary to resolve genuine functional differences between body forms and swimming modes.

Krueger (2006) recently described a similar approach to the one used here. He described a different mechanism for measuring the wake power, which would avoid some of the problems of PIV. In particular, his method would account for all three components of velocity over the entire downstream plane, thus avoiding any assumptions about the 3D structure of the wake. However, he also concludes

that without some other way of estimating thrust, wake power can only be used to provide bounds for the efficiency, in the same way as was done in this study.

4 Conclusions and prospectus

Do trout swim better than eels? This review has demonstrated several problems with both the question itself and a number of ways of evaluating it. First, the question itself is somewhat ill-posed. “Better” depends on the metric used—propulsive efficiency, total power use, or power wasted are important metrics, but they need not all be good under the same conditions. Additionally, swimming performance depends on the conditions under which it is measured. Fig. 7 suggests that eels and trout may waste similar amounts of power—but only when swimming at their preferred speeds. When trout are forced to swim artificially slowly, they seem to be more wasteful than eels. Bluegill, in turn, waste substantial energy during steady swimming (Fig. 7), but, under natural conditions, they rarely swim steadily, so they may not be very well adapted for steady power conservation.

Second, given a particular metric and conditions to measure it, it is still challenging to estimate performance of swimming fishes. Making three-dimensional flow measurements around swimming fishes is not straightforward. In particular, there is no currently feasible method for measuring the flow in a full 3D volume around the swimming fish. PIV, the standard technique, can only measure flow in a plane, although stereo-PIV, which can measure all three components of flow in a plane (Prasad and Adrian 1993; Willert 1997) is becoming more feasible in biological applications (e.g., Nauen and Lauder 2002b). Using stereo-PIV planes perpendicular to the swimming direction as the upstream and downstream boundaries of a control volume would avoid many of the assumptions about 3D flow structure that were necessary in the current analysis.

However, the primary issue is not methodological. Fish are, by definition, self-propelled, which makes it challenging to separate thrust and drag forces (Schultz and Webb 2002). Despite this challenge, there are several avenues remaining to be explored as possible routes for comparing hydrodynamic swimming performance among fishes and underwater vehicles.

1. Temporal separation of forces. Although it was not possible with the limited data used for this review, the fluctuating center-of-mass velocity in carangiform swimmers (Fig. 3) may provide information on the relative magnitude of thrust and drag. In fishes with

relatively large fluctuations in velocity, like the bluegill, the thrust may temporally overwhelm the drag to such an extent that the net force at certain phases in the tail beat cycle is composed primarily of thrust.

2. Spatial separation of forces. Measurements of momentum flux at the tips of the tail may provide information on the thrust force, without much of an effect from the drag on the fish's body (Fig. 5d), particularly in fishes with narrow caudal peduncles like the bluegill sunfish used as an example here, or the mackerel (Nauen and Lauder 2002a) or tuna. Full stereo PIV planes behind the swimming fish, perpendicular to the flow, may provide the best information.
3. Zero-momentum wake profiles. For fishes like the eel, which maintain effectively zero axial momentum in their wakes, the velocity profile in the wake may provide information on the thrust and drag forces simultaneously. The near wake of a self-propelled jet can be used to extract both the individual profiles of thrust and drag wakes (Sirvienta and Patel 2000). Whether the time-average of a highly structured wake from an oscillating propulsor (as in Fig. 4b) can be used in the same way will have to be confirmed by simulations or physical models.
4. Wake power. In the absence of effective methods to extract thrust, the wake power (wasted power), can be used to place bounds on the relative performance of different fishes. Particularly if there are a priori hypotheses about fish performance based on habitat or lifestyle (i.e., that trout are more efficient than eels), the wake power can be used effectively to constrain if not disprove such hypotheses (trout would have to have a surprisingly large drag coefficient to be more efficient than eels, at least at swimming speeds $< 2 L s^{-1}$).

These methods may provide a framework for addressing relative performance as it becomes more feasible to perform comparative studies of swimming in many different fishes.

Comparative studies of the performance of many different fishes, examining many different performance metrics under many different conditions will provide the best route to extracting design principles for undulatory swimming. Only by comparing fishes with different evolutionary histories can one begin to disentangle all the competing adaptive pressures that were involved in producing the body shapes and swimming modes of fishes today. Such comparisons, while challenging, may ultimately provide the best framework for understanding the performance of fishes and biomimetic submarines.

Acknowledgments Many of the ideas in this review developed from a discussion with Rajat Mittal. Data were taken with funding from National Science Foundation grants to George V. Lauder (grant

numbers IBN9807021 and IBN0316675). Support is currently provided by the National Institutes of Health (grant number 5 F32 NS054367).

References

- Afanasyev YD (2004) Wakes behind towed and self-propelled bodies: asymptotic theory. *Phys Fluids* 16:3235–3238. doi:10.1063/1.1768071
- Anderson EJ, McGillis WR, Grosenbaugh MA (2001) The boundary layer of swimming fish. *J Exp Biol* 204:81–102
- Anderson JM (1996) Vortex control for efficient propulsion. Ph.D. Dissertation, Dept Ocean Eng, Mass Inst Tech
- Batchelor GK (1973) An introduction to fluid dynamics. Cambridge University Press, Cambridge
- Breder CM (1926) The locomotion of fishes. *Zoologica* 4:159–297
- Dabiri JO (2005) On the estimation of swimming and flying forces from wake measurements. *J Exp Biol* 208:3519–3532. doi:10.1242/jeb.01813
- Dabiri JO (2006) Note on the induced Lagrangian drift and added-mass of a vortex. *J Fluid Mech* 547:105–113. doi:10.1017/S0022112005007585
- Drucker EG, Lauder GV (1999) Locomotor forces on a swimming fish: three-dimensional vortex wake dynamics quantified using digital particle image velocimetry. *J Exp Biol* 202:2393–2412
- Drucker EG, Lauder GV (2001) Locomotor function of the dorsal fin in teleost fishes: experimental analysis of wake forces in sunfish. *J Exp Biol* 204:2943–2958
- Finson ML (2006) Similarity behaviour of momentumless turbulent wakes. *J Fluid Mech* 71:465–479
- Garland T (1998) Conceptual and methodological issues in testing the predictions of symmorphosis. In: Weibel ER, Taylor CR, Bolis L (eds) Principles of animal design. Cambridge University Press, Cambridge
- Hartel KE, Halliwell DB, Launer AE (2002) Inland fishes of Massachusetts. Massachusetts Audubon Society, Lincoln, MA
- Helfman GS, Collette BB, Facey DE (1997) The diversity of fishes. Blackwell Science, London
- Kern S, Koumoutsakos P (2006) Simulations of optimized anguilliform swimming. *J Exp Biol* 209:4841–4857. doi:10.1242/jeb.02526
- Kipling R (1907) Just so stories. Doubleday, Garden City, NY
- Koochesfahani MM (1989) Vortical patterns in the wake of an oscillating airfoil. *AIAA J* 27:1200–1205
- Krueger PS (2006) Measurement of propulsive power and evaluation of propulsive performance from the wake of a self-propelled vehicle. *Bioinsp Biomimet* 1:S49–S56. doi:10.1088/1748-3182/1/4/S07
- Krueger PS, Gharib M (2003) The significance of vortex ring formation to the impulse and thrust of a starting jet. *Phys Fluids* 15:1271–1281. doi:10.1063/1.1564600
- Lauder GV (2000) Function of the caudal fin during locomotion in fishes: kinematics, flow visualization, and evolutionary patterns. *Am Zool* 40:101–122
- Lauder GV, Tytell ED (2006) Hydrodynamics of undulatory propulsion. In: Shadwick RE, Lauder GV (eds) Fish biomechanics. Academic, San Diego, pp 425–468
- Lighthill J (1960) Note on the swimming of slender fish. *J Fluid Mech* 9:305–317
- Lighthill J (1970) Aquatic animal propulsion of high hydromechanical efficiency. *J Fluid Mech* 44:265–301
- Lighthill J (1971) Large-amplitude elongated-body theory of fish locomotion. *Proc R Soc Lond B* 179:125–138
- McCutchen CW (1977) Froude propulsive efficiency of a small fish, measured by wake visualisation. In: Pedley TJ (ed) Scale effects in animal locomotion. Academic, London, pp 339–363

- Meunier P, Spedding GR (2006) Stratified propeller wakes. *J Fluid Mech* 552:229–256. doi:10.1017/S0022112006008676
- Müller UK, Smit J, Stamhuis EJ, Videler JJ (2001) How the body contributes to the wake in undulatory fish swimming: flow fields of a swimming eel (*Anguilla anguilla*). *J Exp Biol* 204:2751–2762
- Müller UK, van den Heuvel B-LE, Stamhuis EJ, Videler JJ (1997) Fish foot prints: morphology and energetics of the wake behind a continuously swimming mullet (*Chelon labrosus* Risso). *J Exp Biol* 200:2893–2906
- Naudascher E (1965) Flow in the wake of self-propelled bodies and related sources of turbulence. *J Fluid Mech* 22:625–656
- Nauen JC, Lauder GV (2001) Locomotion in scombrid fishes: visualization of flow around the caudal peduncle and finlets of the chub mackerel *Scomber japonicus*. *J Exp Biol* 204:2251–2263
- Nauen JC, Lauder GV (2002a) Hydrodynamics of caudal fin locomotion by chub mackerel, *Scomber japonicus* (Scombridae). *J Exp Biol* 205:1709–1724
- Nauen JC, Lauder GV (2002b) Quantification of the wake of rainbow trout (*Oncorhynchus mykiss*) using three-dimensional stereoscopic digital particle image velocimetry. *J Exp Biol* 205:3271–3279
- Prasad AK (2000) Stereoscopic particle image velocimetry. *Exp Fluids* 29:107–115
- Prasad AK, Adrian RJ (1993) Stereoscopic particle image velocimetry. *Exp Fluids* 15:49–60
- Rosén M, Spedding GR, Hedenstrom A (2004) The relationship between wingbeat kinematics and vortex wake of a thrush nightingale. *J Exp Biol* 207:4255–4268. doi:10.1242/jeb.01283
- Rosen MW (1959) Waterflow about a swimming fish. US Naval Ordnance Test Station, China Lake, CA. Tech Publ 2298, pp 1–96
- Schultz WW, Webb PW (2002) Power requirements of swimming: do new methods resolve old questions? *Integr Comp Biol* 42:1018–1025
- Shames IH (1992) *Mechanics of fluids*, 3rd edn. McGraw-Hill, New York
- Sirviente AI, Patel VC (2000) Wake of a self-propelled body, Part 1: momentumless wake. *AIAA J* 38:611–619
- Spedding GR, Rayner JMV, Pennyquick CJ (1984) Momentum and energy in the wake of a pigeon (*Columba livia*) in slow flight. *J Exp Biol* 111:81–102
- Standen EM, Hinch SG, Rand PS (2004) Influence of river speed on path selection by migrating adult sockeye salmon (*Oncorhynchus nerka*). *Can J Fish Aquat Sci* 61:905–912. doi:10.1139/F04-035
- Standen EM, Lauder GV (2005) Dorsal and anal fin function in bluegill sunfish (*Lepomis macrochirus*): three-dimensional kinematics during propulsion and maneuvering. *J Exp Biol* 208:2753–2763. doi:10.1242/jeb.01706
- Standen EM, Lauder GV (2007) Hydrodynamic function of dorsal and anal fins in brook trout (*Salvelinus fontinalis*). *J Exp Biol* 210:325–339. doi:10.1242/jeb.02661
- Tennekes H, Lumley JL (1972) *A first course in turbulence*. MIT, Cambridge, MA
- Triantafyllou GS, Triantafyllou MS, Grosenbaugh MA (1993) Optimal thrust development in oscillating foils with application to fish propulsion. *J Fluids Struct* 7:205–224
- Tytell ED (2004a) The hydrodynamics of eel swimming. II. Effect of swimming speed. *J Exp Biol* 207:3265–3279. doi:10.1242/jeb.01139
- Tytell ED (2004b) Kinematics and hydrodynamics of linear acceleration in eels, *Anguilla rostrata*. *Proc R Soc Lond B* 271:2535–2541. doi:10.1098/rspb.2004.2901
- Tytell ED (2006) Median fin function in bluegill sunfish, *Lepomis macrochirus*: streamwise vortex structure during steady swimming. *J Exp Biol* 209:1516–1534. doi:10.1242/jeb.02154
- Tytell ED, Ellington CP (2003) How to perform measurements in a hovering animal's wake: physical modelling of the vortex wake of the hawkmoth *Manduca sexta*. *Philos Trans R Soc Lond B* 358:1559–1566. doi:10.1098/rstb.2003.1355
- Tytell ED, Lauder GV (2004) The hydrodynamics of eel swimming. I. Wake structure. *J Exp Biol* 207:1825–1841. doi:10.1242/jeb.00968
- van Ginneken V, Antonissen E, Müller UK, Booms R, Eding E, Verreth J, van den Thillart G (2005) Eel migration to the Sargasso: remarkably high swimming efficiency and low energy costs. *J Exp Biol* 208:1329–1335. doi:10.1242/jeb.01524
- Walker JA (1998) Estimating velocities and accelerations of animal locomotion: a simulation experiment comparing numerical differentiation algorithms. *J Exp Biol* 201:981–995
- Webb PW (1971) The swimming energetics of trout. I. Thrust and power output at cruising speeds. *J Exp Biol* 55:489–520
- Webb PW (1992) Is the high cost of body caudal fin undulatory swimming due to increased friction drag or inertial recoil? *J Exp Biol* 162:157–166
- Webb PW (2006) Stability and maneuverability. In: Shadwick RE, Lauder GV (eds) *Fish biomechanics*. Academic, San Diego, pp 281–332
- Willert CE (1997) Stereoscopic digital particle image velocimetry for application in wind tunnel flows. *Meas Sci Tech* 8:1465–1479
- Willert CE, Gharib M (1991) Digital particle image velocimetry. *Exp Fluids* 10:181–193
- Zhu Q, Wolfgang MJ, Yue DKP, Triantafyllou MS (2002) Three-dimensional flow structures and vorticity control in fish-like swimming. *J Fluid Mech* 468:1–28